Proceedings of the International Conference on Heat Transfer and Fluid Flow
Prague, Czech Republic, August 11-12, 2014
Paper No. 35

Turbulent Flow and Heat Transfer in the Ribbed Divergent Channel

S. W. Ahn, M. S. Lee
Department of Mechanical and System Engineering, Gyeongsang National University
38 Cheondaeguchigil, Tongyeong, Republic of Korea
ahn9294@gnu.ac.kr; regulus84@naver.com

Abstract **-** Heat transfer and friction factors of fully developed turbulent flows in the stationary rectangular divergent channel with parallel angled ribbed have been investigated experimentally. Four different parallel angled ribs (α = 30, 45, 60, and 90-deg)are placed to the channel's two opposite walls as well as to the channel's one sided wall only, respectively. The ribbed rectangular divergent channel has the inclination angle of 0.72deg at the left and right walls, corresponding to D_{ho}/D_{hi} =1.16. The divergent channel has the cross-section of100 x75 mm^2 at inlet and 100 x 100 mm^2 at exit. The ribbed walls are manufactured with a fixed rib height (e) =10 mm and the ratio of rib spacing (p) to height(e) = 10. The measurement was conducted within the range of Reynolds numbers from 15,000 to 89,000.

Keywords**:** Rectangular divergent channel, Parallel angled ribs, Total friction factor, Nusselt number.

1. Introduction

The rib configurations (such as rib height, spacing, angle of attack) and flow Reynolds number on the average heat transfer and pressure drop in the fully developed region of uniformly heated square straight cross sectional channel with two opposite rib-roughened walls were investigated systematically (Han, 1984;Han et al., 1985). The effects of the above parameters on the local heat transfer and pressure drop in developing (entrance) and fully developed regions of foil-heated, ribbed rectangular straight channels with five different aspect ratios were reported (Han, 1988;Han and Park, 1988). The results show that the angled ribs provide a better heat transfer performance than the transverse ribs, and the narrow aspect ratio channels (near the leading edge of the airfoil) perform better than the broad aspect ratio channels (near the trailing edge of the airfoil). Effects of the four different rib-angle orientations on the local mass transfer and pressure drop distributions in the rectangular straight channels have also been reported (Chandra et al., 1997). These previous studies show that rib angle orientation on the walls of a cooling straight channel has a significant impact on the local heat transfer and pressure drop distributions. However, no significant study was found in the existing literature that dealing with heat transfer in the ribbed convergent and divergent channels. Hu and Shen (1996) investigated the heat transfer enhancement in a converging passage with discrete ribs. The test was performed with staggered array of 45oangled discrete ribs, and also with a combination of the discrete ribs with groove on two opposite walls of the passage. The area-averaged enhancement factors of 3 to 4 and 2.5 to 3.2 were obtained, respectively, for both promoter configurations studied. The data was presented as contours of enhancement factors. Our previous work (Lee et al., 2013) conducted an investigation of local heat transfer and pressure drops of developed turbulent flows in the stationary rectangular convergent and divergent channels with transverse ribs on one-sided surface only. The rectangular convergent and divergent channels have the inclination angles of 0.72 and 1.42-deg at the two opposite walls only. The results show that among the four channels of the ratios of the hydraulic diameter at exit to the hydraulic diameter at inlet (D_{ho}/D_{hi}) =0.67, 0.86, 1.16 and 1.49, the channel with the (D_{ho}/D_{hi})=1.16 has the highest thermal performance at the identical pumping power and static pressure drop. This current study tries to address a pertinent industrial issue by quantifying the effects of angled ribs on the wall in the rectangular divergent channel. Since the industrial turbine airfoil cooling channels have usually the convergent and

divergent configurations, a study documenting the effects of angled ribs on heat transfer and friction factors in the convergent and divergent channels could be proved of great value of engine designers. The objective of this study is to measure heat transfer coefficients and friction factors for the divergent channel of D_{ho}/D_{hi} =1.16 with 30, 45, 60 and 90-deg parallel angled ribs on the one wall and two opposite walls, respectively.

2. Experimental Apparatus and Data Reduction

The experimental program used in the study was described in some detail in ref. (Lee et al., 2013). A brief introduction is presented here to clarify the configuration parameters that related to the present study. The forced air goes through a honeycomb, an entrance section of 2.5 m long, a test section of 1 m long, and a 76.2 mm diameter, 1.4 m length pipe, equipped with multiport averaging Pitot tube measure the flow rate. The rectangular divergent test section has the cross sections of 100 x75 mm^2 at the inlet and 100 x 100 mm^2 at the exit, which corresponding to the hydraulic diameter ratio (D_{ho}/D_{hi}) of 1.16 and the divergence at the left and right side walls only. The rib size and arrangement are presented in Fig. 1, at which the dimension of a fixed rib is height (e) of 10 mm and width of 5 mm, and the ratio of rib spacing (p)/height (e) =10. The rib height to hydraulic diameter ratio (e/D_h) of 0.117 is used. Four different parallel rib angles, α =30, 45, 60 and 90-deg are considered. Each of left and right side walls is subdivided into 10 sub-sequential stream-wise regions, each comprising 1 copper plate (100 mm x 100 mm). The angled ribs are placed in parallel are attached on the left wall only, as well as on both of the left and right walls, respectively. The other opposite walls (top and bottom) are left smooth. Ribs are made of copper and attached to the copper plates using 0.05 mm thick double sided tape. In order to obtain the local heat transfer coefficients, The left and right walls in the test channel were uniformly heated by passing a current through 0.1 mm thick silicone heaters cemented separately to the back of each wall (left and right ribbed walls), and the top and bottom wall are insulated. The power input can be varied by controlling a single phase transformer and measuring the voltage applied to the heater by a digital multi-meter. Each copper plate is instrumented with T-type copper-constantan thermocouples; the left and right copper plates have 2 thermocouples each. The thermocouples are buried inside a 0.4 mm diameter hole drilled on the plates and held in place by using a high conductivity epoxy resin. These thermocouples are connected to a Yokogawa DA 100. The test section is insulated within a 50 mm thick pine wood housing. The thermocouples were calibrated in advance and their accuracy is estimated to be about 0.2°C. Further insulation is provided by encapsulating the entire test section in a thick layer of glass wool. 12 pressure taps are set up at the same interval along the top smooth wall centerline. Static pressure is measured using either an inclined manometer or a digital micro-manometer with a resolution up to 0.01 mmH_2O at the static pressure 19.99 mmH_2O, depending on its value. An uncertainty estimation was conducted as suggested by Kline and McClintock (1953). The maximum uncertainty in the average Nusselt number was estimated to be less than 11 % and that for the friction factor less than 12%.

The micro-manometer connected to pressure taps measures the static pressure drop (P_i-P_o) along the stream-wise direction on the smooth top wall. The tested Reynolds number covered is from 15,000 to 89,000, approximately. The pressure and temperature of the ambient are also recorded before each run. The general friction factor (f) and total friction factor (f_T) of the divergent channels are defined as:

$$f = \frac{D_h}{2\rho u_b^2}|\Delta P/L| \quad (1)$$

$$f_T = \frac{D_h}{2\rho u_b^2}|\Delta Pe/L| \quad (2)$$

Where the static pressure difference ΔP is P_i-P_o and total pressure difference ΔPe is P_i-P_o + $\frac{1}{2}\rho u_{bi}^2$-$\frac{1}{2}\rho u_{bo}^2$. The channel average velocity u_b stands for (u_{bi}+u_{bo})/2. The subscripts i and o mean the inlet and exit of test section, respectively. L indicates the length of test section. As for the most cases of the internal convective heat transfer, the fluid properties are evaluated at the mean temperature of the fluid in the channel. The Reynolds number is defined as:

$$Re = \frac{u_b D_h}{\nu} \tag{3}$$

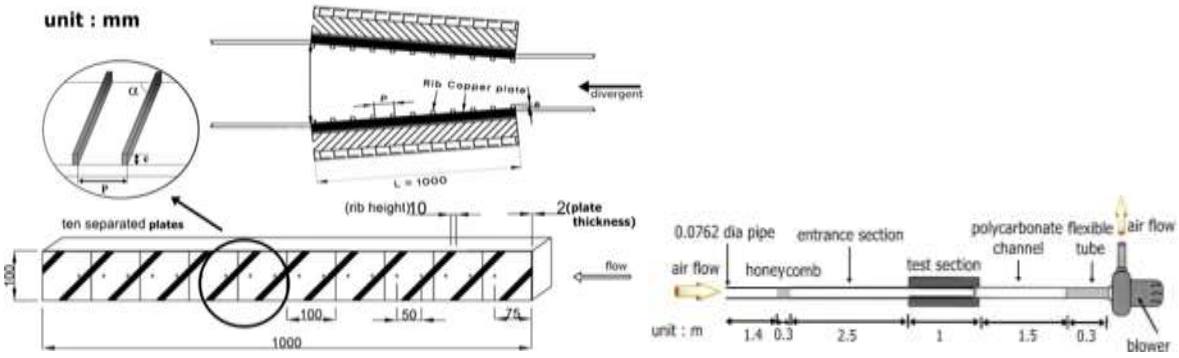

Fig. 1. Test section.

The local heat transfer coefficient h_x was calculated from the local net heat transfer rate per unit projected surface area (*A*) to the cooling air, the local wall temperature on each copper plate, and the local bulk mean air temperature in terms of Newton's Law of Cooling as:

$$h_x = \frac{(Q - Q_{loss})}{A(T_{w,x} - T_{b,x})} \tag{4}$$

Eq. (4) was used for the local ribbed side wall and smooth side wall heat transfer coefficient calculations. To place the results on a common basis, the heat transfer area used in Eq. (4) was always that of a smooth wall. The net rate of heat transfer is determined from the difference of power supplied to each heater and the heat lost from the test section. The heat loss to the environment is calibrated for based on a heat loss test. The test section (with all insulation in place and its interior filled fiberglass) is heated until a steady state temperature is reached. The heat supplied at the steady state is equal to the heat leakage through the external insulation. This test is conducted for two steady states, corresponding to the highest and lowest temperatures expected in the experiment. The local bulk temperature $T_{b,x}$ is computed by interpolating the exit and inlet bulk temperatures. The bulk temperature difference (T_{bi}- T_{bo}) between the inlet and exit of test section was 3.7°C in the channel with two opposite 60-deg angled ribbed walls at the Reynolds number of 36,000. The channel average Nusselt number was defined as:

$$Nu = h\, D_h/k \tag{5}$$

Where *h* is the channel average convective heat transfer coefficient

3. Result and Discussion

The static pressure drops at the test section are plotted with Reynolds number in Fig. 2 for various tested rib angles. The static pressure drops (P_i-P_o) are calculated by fitting a straight line into the data points taken 12 a time and taking the slope of this line as the (P_i-P_o) along the centerline of the test section.

In this figure, the open symbol stands for one sided ribbed wall channel and the solid symbol stands for two opposite ribbed wall channel. It is found from the experimental raw data that the two opposite wall channel produces about 2.1 times greater negative static pressure drops than in the one sided ribbed wall channel at the flow attack angle (α) of 60-deg and Reynolds number of 84,000. Fig. 2 compares the static pressure drops (P_i-P_o) between parallel rib attack angles of 30, 45, 60 and 90-deg with e/D_h=0.117 and p/e=10 for the one-sided ribbed wall channel and the two opposite ribbed wall channel, respectively. The results show that the 45-deg parallel ribs provide the greatest negative static pressure drops at the one sided ribbed wall; however, the 90-deg parallel ribs have the greatest static pressure drops at the two opposite walls. It is conjectured that the 45-deg parallel ribs induce a violent secondary flow swirl on the

ribbed side and toward the smooth side wall in the one sided ribbed wall channel, this secondary flow interferes the main stream flow; however, in the channel with the two opposite ribbed walls, the transverse ribs (90-deg) produce the greatest static pressure drops because of the greatest flow blockage.

The interesting feature of the general friction factors of the present study can be seen that, on the contrary to the public opinion, the friction factors of 30-deg angled ribs on the one sided ribbed channel walls (open square symbols) are lower than those for what was predicted by Blasius' equation (6) for the smooth circular tube. This may be caused by the decrease in the static pressure drop induced by the inclined wall.

The total friction factors obtained from equation (2) is shown in Fig. 3, along with results by our previous work (Lee et al., 2013). The increase in the total friction factors can be seen in the order of 90, 30, 60, and 45-deg in the two opposite ribbed wall channel and 30, 90, 60, and 45-deg in the one sided ribbed wall channel. It is attributed to the fact that the total friction factors are determined from the total pressure drops, corresponding to the combination of the static pressure drops of Fig. 2 and the dynamic pressure drops. The friction factor f_{ss} of Eq. (6) for the fully developed turbulent flow in the smooth circular tube proposed by Blasius is included as a reference.

$$f_{ss} = 0.046Re^{-0.2} \quad (6)$$

Our previous work (Lee et al., 2013) with one ribbed wall of D_{ho}/D_{hi}=1.16 (dotted line) provides somewhat higher total friction factor than in the present one ribbed wall channel with flow attack angle of 90-deg (open diamond symbols). It is reasoned that the channel hydraulic diameter (D_h) is defined as D_{ho} in our previous work.

The Reynolds number dependencies of the local centerline convective heat transfer coefficient for four different parallel angled ribs in the channel with one sided ribbed wall are shown in Fig. 4. By careful examination of these figures, we may find the following characteristics: 1) For all the parallel angled ribbed channels, the local heat transfer coefficients show a monotonically increasing trend with the Reynolds number, with the increasing ratio of the 45-deg angled ribs being the highest at the mid test section. 2) It should be noted that the local heat transfer coefficient in the region close to the test section exit exhibits an increasing trend. This is expected to have resulted from the end heat loss, which makes the wall temperatures nearby decrease to some extent. The guided-heating method (an additional heating element was used after the test section to balance the axial heat conduction from the test section) should have been adopted to alleviate such a phenomenon. 3) The local heat transfer coefficient keeps continuously decreasing along the stream-wise distance at the 90-deg angled ribs, while for the 30, 45, and 60-deg angled ribs, the local heat transfer coefficient keeps al produce the secondary flows, and therefore promote strongly the local heat transfer coefficient. most constant except for the regions of inlet and exit of test section. This suggests that the parallel angled ribs could produce the secondary flows, and therefore promote strongly the local heat transfer coefficient.

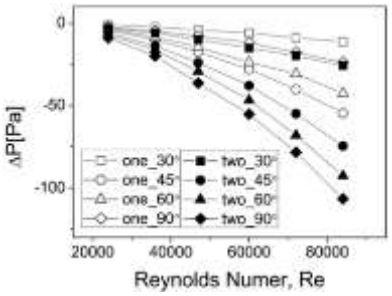

Fig. 2. General friction factor.

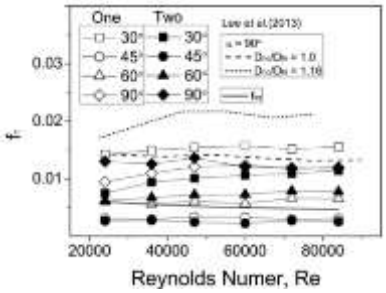

Fig. 3. Total friction factor.

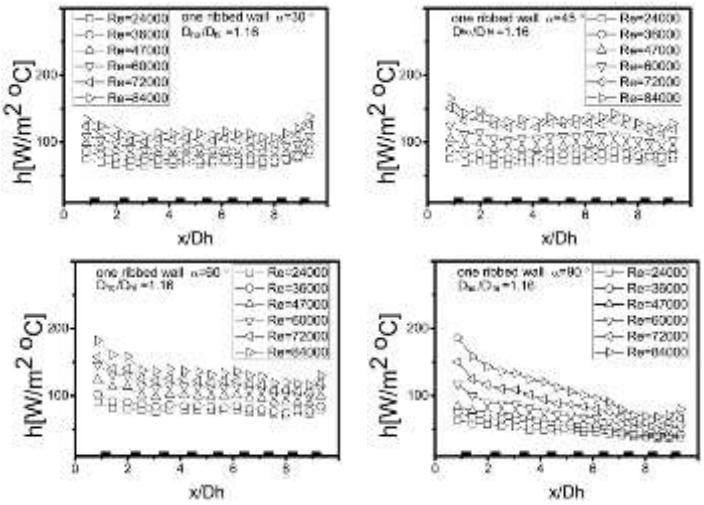

Fig. 4. Local heat transfer coefficient with one sided ribbed wall.

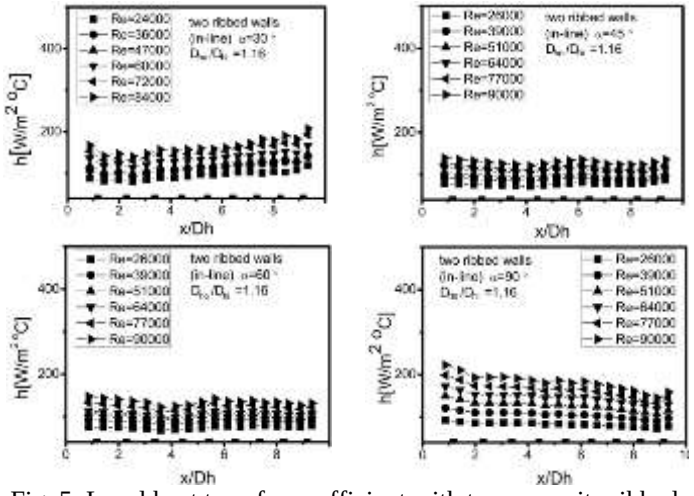

Fig. 5. Local heat transfer coefficient with two opposite ribbed.

Fig. 5 is the local convective heat transfer coefficient for the channel with two opposite ribbed walls. On contrary to Fig. 4, for the 30-deg angled ribs the local convective heat transfer coefficient keeps continuously increasing along the stream-wise distance except the thermal entrance while for the 90-deg angled ribs, the local convective heat transfer coefficient keeps continuously decreasing at the slower slope than in the one ribbed wall channel. This is because the 90-deg angled ribs break up the laminar sublayer and create local wall turbulence due to flow separation from the ribs and reattachment between the ribs. Thus, the more turbulence is experienced in the two opposite ribbed wall channel. This leads to the fact that the two opposite ribbed wall heat transfer coefficients are higher than the one sided ribbed wall heat transfer coefficients. At the 45 and 60-deg angled ribs in Fig. 5, the heat transfer coefficients increase abruptly and then diminish at x/D_h of 6. It is reasoned that the secondary flow from the parallel angled ribs may promote the turbulent swirl in the channel.

In the straight cross sectional channel (Park et al.,1992), the parallel angled ribs on the walls may induce secondary flow (or swirling flow) along the rib axes. Therefore, the local convective heat transfer coefficients increase along the stream-wise distance after developing flow region, whereas the local heat transfer coefficients decrease or stay constant except for the 30-deg angled ribs in the present channel.
The different stream-wise variation patterns of the local heat transfer coefficients between the straight channel and present divergent channels are obviously caused by the stream-wise flow deceleration, as revealed by previous investigation (Succec and Lu, 1990).

The channel average Nusselt number versus the Reynolds number is shown in Fig. 6, along with results by (Chandra et al, 1997; Lee et al, 2013). The present channel average Nusselt number with two opposite ribbed walls is somewhat higher than in the straight cross sectional channel (Chandra et al, 1997). This could be attributed to two reasons. First, the divergent channel produces the flow deceleration, which leads the air bulk temperature increase and an increase in the Nusselt number to some extent. Second, the present Nusselt number is defined as(hD_h)/k with D_h =(D_{hi}+D_{ho})/2 rather than D_{hi}.

The present one ribbed wall channel of D_{ho}/D_{hi}=1.16 with flow attack angle of 90-deg (open diamond symbols) produces a little lower Nusselt number than in our previous data (dotted and dashed line)(Chandra et al, 1997). It is postulated that the present Nusselt number is defined as (hD_h)/k with D_h=(D_{hi}+D_{ho})/2 as opposed to D_h = D_{ho} at our previous work.

The centerline Nusselt numbers with angled ribs of 45 and 60-deg are higher than those with transverse ribs (90-deg) in the one ribbed wall channel, whereas the Nusselt numbers with the 90-deg ribs are higher than the 45 and 60-deg ribs in the two opposite ribbed wall channel.

Park et al. (1992) showed a comparison of heat transfer and friction factor with different parallel rib angles (30, 45, 60, and 90-deg) in different aspect ratio (W/H=1/4, 1/2, 1, 2, and 4) straight channels with a relatively lower rib height of e/D_h=0.047 on two opposite walls. They concluded that the 90-deg orthogonal ribs give the lowest heat transfer and pressure drop in narrow aspect ratio (W/H=1/4), and the 60-deg parallel angled ribs provides the highest heat transfer and pressure drop in the square channel (W/H =1), whereas the 90-deg ribs produces the highest heat transfer and pressure drop in the broad-aspect ratio channel(W/H =4) with ribs on the two opposite broad walls, corresponding to the worst air flow blockage. Unlike a 90-deg rib, the 60 and 45-deg angled rib orientation cause a drop in the heat transfer and pressure drop for W/H =4. This is similar trend with Figs. 5 and 8 with e/D_h=0.117that the 60 and 45-deg angled ribs give the higher heat transfer and pressure drop in the one ribbed wall divergent channel with relatively weaker air flow blockage that in the 90-deg rib, but the 90-deg transverse rib gives the higher heat transfer and pressure drop in the two opposite ribbed wall divergent channel with the relatively worse air flow blockage.

It is possible that the angled ribs (60 and 45-deg) act as flutes in the two opposite ribbed wall channel with the worse air flow blockage to create mostly a swirl in the flow. Therefore, the boundary layer separation effect is weaker than the swirl generated by the parallel angled rib.

Considering Figs. 3 and 6, the total friction factor in the present divergent channel with one 90-deg ribbed wall (open diamond) is somewhat lower than in the straight cross sectional channel (dashed line) (Lee, et al., 2013); however, the Nusselt number (open diamond symbols) is a little greater than in the straight cross sectional channel (dashed line).

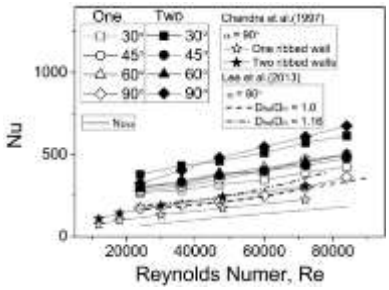

Fig. 6. Channel average Nusselt number.

This is the contrary to the Reynolds analogy (Holman, 1997) between heat transfer and fluid friction that the Nusselt number is proportional to the friction factor. The present parallel ribbed divergent channel of D_{ho}/D_{hi}=1.16 is confirmed to be a better design than in the ribbed straight cross sectional channel. The Nusselt number Nu_{ss} for the fully developed smooth circular tubes correlated by Dittus-Boelter (1930) is included as a reference.

4. Conclusions

Pressure drop and heat transfer measurements have been performed in the divergent channels with the parallel rib angles of 30, 45, 60 and 90-deg for the Reynolds numbers from 15,000 to 89,000. The main findings of the study are given below:

1. The 45deg parallel ribs provide the greatest negative static pressure drop at the one sided ribbed wall; However, the90-deg parallel ribs have the greatest static pressure drops at the opposite ribbed walls.
2. The total friction factors in the present 90-deg angled ribbed divergent channels are somewhat lower than in the straight ribbed cross sectional channels (Lee et al., 2013); however, the Nusselt numbers are a little greater than in the ribbed straight cross sectional channels.
3. The increases in the Nusselt numbers for the flow attack angles can be seen in the order of 90, 30, 60 and 45-deg at the two opposite ribbed divergent wall channels.

Acknowledgments

This research was supported by Basic Science Research Program through the National Research Foundation of Korea(NRF) funded by the Ministry of Science, Education, Science and Technology(grant number: 2012001401).

References

Chandra, P. R., Niland, M. E. and Han, J. C. (1997). Turbulent flow heat transfer and friction in a rectangular channel with varying numbers of ribbed walls, Journal of Turbomachinery, 119, 374-380.

Dittus, F. W. and L. M. Boelter, L. M. (1930). University of California (Berkeley) Publications in Engineering 2, Berkeley, pp. 443 – 461.

Han, J. C. (1984). Heat transfer and friction in channels with two opposite rib-roughened walls, Journal of Heat Transfer. 106, 774-781.

Han, J. C. (1988). Heat transfer and friction characteristics in rectangular channel with rib turbulators, Journal of Heat Transfer, 110, 321-328.

Han, J. C. and Park, J. S. (1988). Developing heat transfer in rectangular channels with rib turbuators, International Journal of Heat Mass Transfer, 31, 183-195.

Han, J. C., Park, J. S. and Lei, C. K. (1985). Heat transfer enhancement in channels turbulence promotors, Journal of Engineering Gas Turbine Power, 107, 628-635.

Holman, J. P. (1997). Heat Transfer, 8th ed., McGraw-Hill Inc., NewYork , 218-282.

Hu, Z. and Shen, J. (1996). Heat transfer enhancement in a converging passage with discrete ribs, International Journal of Heat Mass Transfer, 39, 1719-1727.

Kline, S. J. and Mclintock, F. A. (1953). Describing uncertainties in single sample experiments, Mechanical Engineering, 75, 3-8.

Lee, M. S., Jeong, S. S., Ahn, S. W. and Han, J. C. (2013). Heat transfer and friction in rectangular convergent and divergent channels with ribs, AIAA J. Thermophysics and Heat Transfer, 27, 660-667.

Park, J. S., Han, J. C., Huang, S. Ou and Boyle, R. L.(1992). Heat transfer performance comparisons of five different rectangular channels with parallel angled ribs, International Journal of Heat Mass Transfer, 35, 2891-2901.

Succec, J. and Lu, Y. (1990). Heat transfer across turbulent boundary layers with pressure gradients, Journal of Heat Transfer, 112, 906-912.